DESIGN, SYNTHESIS, CHARACTERIZATION, BIOACTIVITY AND MOLECULAR DOCKING STUDIES OF NOVEL SULFAMIDES

Ali NADERI[a], Akın AKINCIOĞLU[b,c], Ahmet ÇAĞAN[b], Süleyman GÖKSU[a]*, Parham TASLIMI[d], İlhami GÜLÇIN[a]

ABSTRACT. Starting from commercially available 4-phenylbutanoic acids, a series of novel sulfamides were synthesized and investigated for their inhibition properties on the human carbonic anhydrase I and II (hCA I and II), acetylcholinesterase (AChE) and butyrylcholinesterase (BChE) enzymes. SAR was also evaluated with molecular docking study. These new compounds were tested against hCA I and hCA II, BChE, and AChE. The majority of the synthetic compounds were more effective against AChE than tacrine, a common inhibitor. Additionally, tacrine was not the only synthetic substance that was more effective against BChE. The obtained results revealed that *N,N*-dimethyl-[3-(2,4-dimethoxyphenyl)propyl]sulfamide **25**, with K_i of 94.22±42.37 nM against AChE and K_i of 230.91±46.22 nM against BChE, was the most potent compound against cholinesterase enzymes. These recently created substances were tested for their ability to inhibit hCA I and II isoforms. In comparison to the conventional inhibitor acetazolamide, the majority of produced sulfamide derivatives **25–29** also inhibited these investigated isoforms. In particular, sulfamide derivatives **25-29** with substituents *N,N*-dimethyl-[3-(3,5-dimethoxyphenyl)propyl]sulfamide **26** and N,N-dimethyl-[3-(3,4-dimethoxyphenyl)propyl]sulfamide **27** emerged as the most potent hCA inhibitors.

Keywords: Synthesis; 3-phenylbutylamine; sulfamide; biological effects; molecular docking

[a] *Atatürk University, Faculty of Science, Department of Chemistry, Erzurum, TURKIYE*
[b] *Ağrı İbrahim Çeçen University, Central Researching Laboratory, 04100-Agri, TURKIYE*
[c] *Ağrı İbrahim Çeçen University, Vocational School, 04100-Agri, TURKIYE*
[d] *Department of Biotechnology, Faculty of Science, Bartın University, 74100-Bartin, TURKIYE*
* *Corresponding author: sgoksu@atauni.edu.tr*

ALI NADERI, AKIN AKINCIOĞLU, AHMET ÇAĞAN, SÜLEYMAN GÖKSU,
PARHAM TASLIMI, İLHAMI GÜLÇIN

INTRODUCTION

Sulfamides are of great importance due to their use in synthetic organic chemistry, pharmaceutical chemistry, agriculture and material [1]. The potentially important pharmacological properties of the sulfamide functional group have led to the exhibit of a wide range of biological activities. Anti-cancer activity [2], HIV protease inhibition [3], β3-adrenergic receptor agonist properties [4], γ-secretase inhibition [5], Factor Xa inhibition [6], Norwalk virus inhibition [7], antimicrobial properties [8], human skin chymase inhibition [9], thrombin inhibition [10] and carbonic anhydrase inhibition (CA) [11] of sulfamide compounds have been reported in the literature. Because of these diverse activities, some small molecules including sulfamide moiety have been developed and appeared in the markets as drugs. Histamine H_2 receptor antagonist drug Famotidine (Pepcid, **1**) is used in the treatment of gastroesophageal reflux disease, peptic ulcer disease, and Zollinger-Ellison syndrome [12]. A selective dopamine D_2 receptor agonist drug Quinagolide (Norprolac, **2**) is used for the treatment of hyperprolactinemia [13]. Macitentan (Opsumit, **3**) was developed by Actelion. It is an endothelin receptor antagonist used for the treatment of pulmonary arterial hypertension [14]. A member of the carbapenem class of antibiotics, doripenem (Doribax, Finibax, 4) is a lactam with a wide range of bacterial sensitivity, including both gram-positive and gram-negative bacteria [15] (Figure 1).
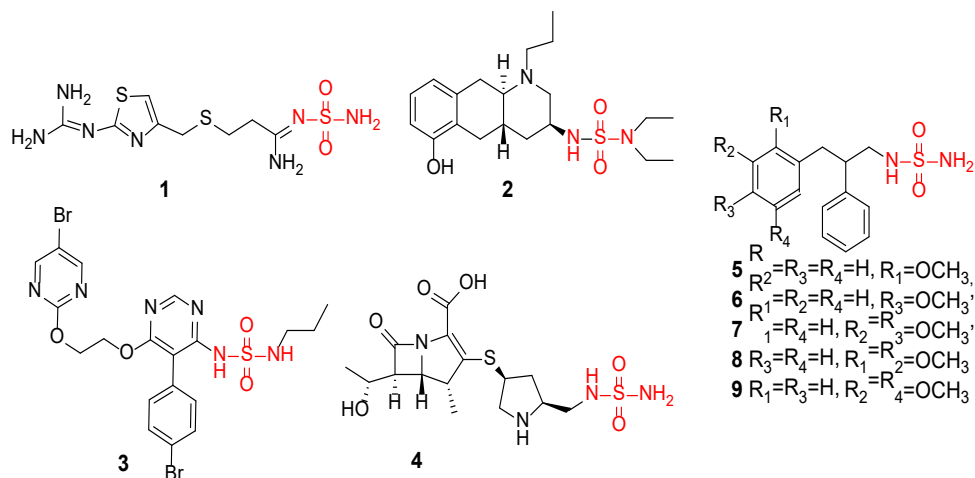

Figure 1. Sulfamide drugs **1-4** and bioactive compounds **5-9**.

Because of the significant biochemical activities of sulfamides, our research group has also synthesized a series of compounds containing sulfamide groups within the scope of drug discovery research. In one of these studies, we reported the synthesis, hCA, AChE, and BChE inhibition of sulfamides **5-9** derived from β-benzylphenethylamines [16]. Additionally, hCA, AChE and BChE inhibitory properties of sulfamide derivatives of benzylamines [17,18], acetophenones [19], dopamine analogues [20,21], 1-aminoindanes and 1-aminotetralins [22], 2-aminoindanes and 2-amino tetralins have also been reported by us [23-25].

Carbonic anhydrases (CAs) are classified in eight different families including α-, β-, γ-, δ-, ζ-, η-, θ-, and t-Cas [26]. Among them, α-CAs is found in all mammals and human. α-CAs include sixteen distinct and different isoforms, which catalyze the transformation of carbon dioxide (CO_2) into bicarbonate (HCO_3^-) ions. Each of human CA has a unique role and location within the body [27]. This relates to how hCA variations are relevant to a number of illnesses, including epilepsy, glaucoma, mountain sickness, osteoporosis, ulcers, obesity, and cancer [28]. Two of the sixteen mammalian CAs that are known are hCA I and hCA II. Red blood cells are where both variations are mostly produced and detected [29,30]. Despite having only 60% sequence homology, they have homologous 3D structures. hCA I and II coordinate a zinc ion in their active form, similar to the majority of the CAs. With a $kcat/K_M = 1.5 \times 10^8$ $M^{-1}s^{-1}$ for the conversion of carbon dioxide (CO_2) to bicarbonate, hCA II is one of the most effective enzymes currently known, but hCA I has a lower efficiency with a $kcat/K_M = 5 \times 10^7$ $M^{-1}s^{-1}$ for the same process [31,32].

Major neuro cognitive abnormalities are most frequently caused by Alzheimer's disease (AD), which affected roughly 5.7 million people in the US in 2018. It is essential to assess the safety and efficacy of the current available treatment regimens given that the illness burden is predicted to rise significantly in the coming years [33]. Since its introduction in 1993, cholinesterase inhibitors (ChEIs) have remained essential in treating the signs and symptoms of AD and may even be able to decrease its progression [34]. A frequent assessment of the safety and effectiveness of administering these medications is necessary due to the fact that they are a mainstay in the treatment of AD, particularly with the approval of new formulations and doses [35]. BChE has an important role in cholinergic mediation [36]. In addition, it has been reported that it has a detoxifying effect against different xenobiotic drugs such as cocaine, succinylcholine, mivacurium, procaine and
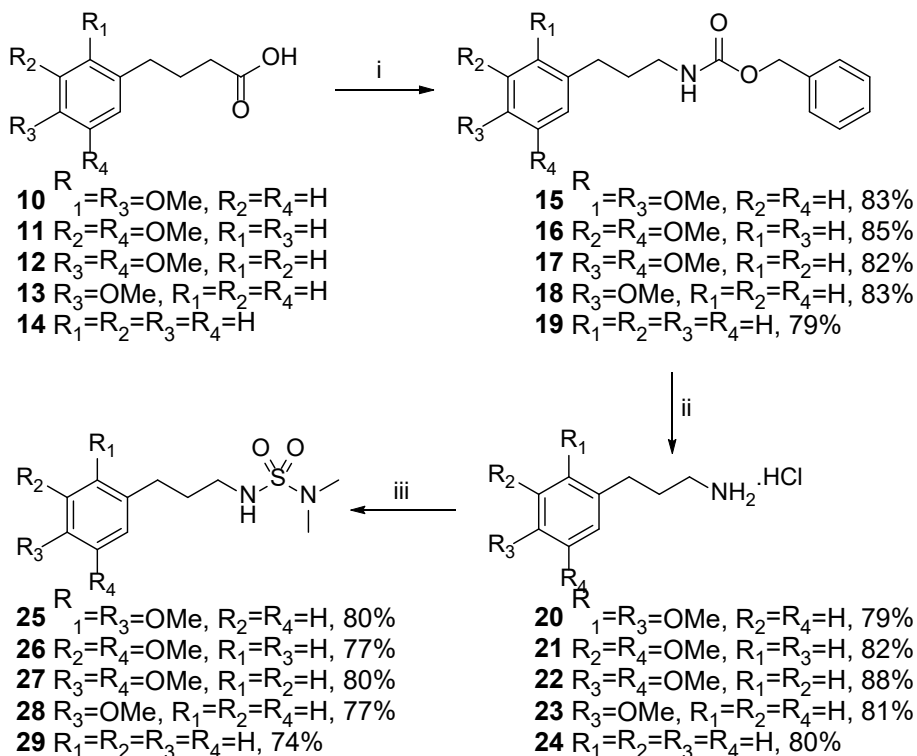
heroin, thus contributing to neurogenesis. It is also assumed that BChE takes over the function of AChE in case of any failure or in later stages of AD as the most common neurodegenerative disease [37,38].

As can be seen from the description given above, the synthesis of novel sulfamides and investigation of their biological properties is very precious for the development of new pioneers of drug-active substances. When the biological properties of compounds **5-9** that are sulfamide derivatives of 2,3-diphenylpropylamines was taken in consideration, the synthesis of sulfamide derivatives of substituted propyl amines will be important for the structure activity relationships of target enzymes hCA, AChE and BChE. In this context, we aimed the synthesis of some novel sulfamides derived from 3-phenylpropylamines and investigation of their hCA, AChE, and BChE inhibitory properties, as well as their structure-activity relationship (SAR) and ADME properties.

RESULT AND DISCUSSION

Chemistry

Our synthesis is based on commercially available 4-phenylbutanoic acid derivatives **10**, **11**, **12**, **13** and **14.** The Curtius reaction of carboxylic acids **10-14** was carried out with diphenylphosporyl azide (DPPA) in dry toluene at 110°C for 4 hours. Then the addition of benzyl alcohol to the reaction mixture and continuation of the reaction at 110°C for 48 hours afforded carbamates **15-19** in high yields (83-85%). Benzyloxy carbamates are easily giving amine hydrochloride salts via Pd-C catalyzed hydrogenolysis in MeOH-CHCl$_3$ at 25°C [39]. Applying of the same method to carbamates **15-19** produced 3-phenylpropylamine hydrochloride salts **20-24** in good yields (79-88%). Amines are giving their sulfamide derivatives from the reactions with *N,N*-dimethysulfamoyl chloride. The reaction of amine hydrochloride salts **20-24** with *N,N*-dimethysulfamoyl chloride in the presence of NEt$_3$ in CH$_2$Cl$_2$ at 25°C gave desired novel sulfamides **25-29** with the yields ranging from 74% to 80% (Scheme 1).

10 $R_1=R_3=$OMe, $R_2=R_4=$H
11 $R_2=R_4=$OMe, $R_1=R_3=$H
12 $R_3=R_4=$OMe, $R_1=R_2=$H
13 $R_3=$OMe, $R_1=R_2=R_4=$H
14 $R_1=R_2=R_3=R_4=$H

15 $R_1=R_3=$OMe, $R_2=R_4=$H, 83%
16 $R_2=R_4=$OMe, $R_1=R_3=$H, 85%
17 $R_3=R_4=$OMe, $R_1=R_2=$H, 82%
18 $R_3=$OMe, $R_1=R_2=R_4=$H, 83%
19 $R_1=R_2=R_3=R_4=$H, 79%

25 $R_1=R_3=$OMe, $R_2=R_4=$H, 80%
26 $R_2=R_4=$OMe, $R_1=R_3=$H, 77%
27 $R_3=R_4=$OMe, $R_1=R_2=$H, 80%
28 $R_3=$OMe, $R_1=R_2=R_4=$H, 77%
29 $R_1=R_2=R_3=R_4=$H, 74%

20 $R_1=R_3=$OMe, $R_2=R_4=$H, 79%
21 $R_2=R_4=$OMe, $R_1=R_3=$H, 82%
22 $R_3=R_4=$OMe, $R_1=R_2=$H, 88%
23 $R_3=$OMe, $R_1=R_2=R_4=$H, 81%
24 $R_1=R_2=R_3=R_4=$H, 80%

Scheme 1. Synthesis of phenathylamine derivatives and *N,N*-dimethyl substituted sulfamide derivatives; i) DPPA/NEt$_3$, BnOH, toluene, 0-110ºC, 52 h; ii) H$_2$/Pd-C, CHCl$_3$-MeOH, 25ºC, 12 h; iii) (CH$_3$)$_2$NSO$_2$Cl, NEt$_3$, CH$_2$Cl$_2$, 25ºC, 8 h.

Bioactivities

Tacrine, also known as 9-amino-1,2,3,4-tetrahydroaminoacridine, is a mildly selective, reversible, non-competitive cholinesterase inhibitor that inhibits both AChE and BChE. Tacrine's main result is a stronger, more reversible suppression of BChE than AChE. The level of ACh in the CNS is hypothesized to rise as a result of this inhibition. By inhibiting potassium channels and lengthening the time the action potential lasts, tacrine also lengthens the time ACh is released from cholinergic neurons [40,41]. The four AChEIs donepezil, rivastigmine, galantamine, and tacrine as well as the NMDA receptor antagonist memantine are currently the only therapies for AD [42-44]. The anti-cholinesterase effects of novel sulfamide derivatives (**25–29**) and tacrine, a positive control, were assessed using Ellman's method [45]. Table 1 lists

the IC_{50} and K_i values for the novel sulfamide derivatives' inhibitory effects against AChE and BChE. As observed in Table 1, all new synthesized compounds **25**, **26**, **27**, **28**, and **29** were more potent than tacrine against AChE while all the synthesized compounds were more potent than the latter drug against BChE. Increased AChE inhibition is closely linked to the pathology of some diseases including Alzheimer's disease, dementia with Lewy bodies, Myasthenia gravis, and glaucoma. It is known that abnormal BChE inhibition is associated with many diseases, including diabetes, cardiovascular diseases, metabolic syndrome, hepatocellular carcinoma, chronic liver disease, postoperative delirium as well as organophosphate and metal poisoning [46]. In the tested compounds, compound of **25**, which possessed two methoxy groups ($-OCH_3$) at *meta* position in the phenolic ring, had the most effective inhibition against AChE. The inhibitory ability was drastically reduced when hydrogen was replaced with o methoxy or when the position of the hydrogen substituent in the methoxy position was changed, as in compounds **25** and **29**, respectively. Contrarily, compounds **25** and **29** (the second powerful molecule) showed a considerable increase in inhibitory ability when the methoxy group was replaced with hydrogen, particularly with the methoxy group. The compound **26** was the third-most effective chemical towards AChE. Notably, the fourth most effective molecule against AChE was the other hydrogen and methoxy derivative **27**. The hydrogen and methoxy substituent in compound **28** made it among the remaining compounds more effective than tacrine (Table 1). All of the produced compounds, particularly those with methoxy group substituents, had outstanding inhibitory action in comparison to tacrine when it came to the anti-BChE ability of novel sulfamide derivatives **25–29** (Figure 2).

Table 1. Structures and cholinesterase inhibitory ability of new sulfamide derivatives **25-29**.

Compound	IC_{50} (nM)				K_i (nM)	
	AChE	r^2	BChE	r^2	AChE	BChE
25	203.63	0.96	659.37	0.99	94.22±42.37	230.91±46.22
26	226.76	0.97	695.78	0.98	109.92±37.53	276.70±34.02
27	204.36	0.98	825.97	0.97	190.67±74.26	328.44±58.58
28	272.08	0.97	794.72	0.96	198.60±73.98	279.24±58.64
29	202.40	0.95	1025.14	0.98	105.06±46.15	378.36±39.60
Tacrine	837.96	0.98	1526.43	0.97	620.12±26.05	809.25±146.60

Inhibitory effect against hCA I and hCA II isoforms

Among the sixteen known hCA isoforms, hCA II is the main physiologic isoform. It is more important than the other 12 catalytically active hCA isoforms in the regulation of intraocular pressure because of its high availability in the various anatomical and cellular areas of the eye, such as the retina and lens [47]. The brain, kidney, gastric mucosa, osteoclasts, RBCs, skeletal muscle, testes, pancreas, lungs, and other organs and tissues also contain this isoform [48]. Earlier, systemically administered hCA II inhibitors for the treatment of glaucoma were created based on sulfonamides like dichlorphenamide, methazolamide, acetazolamide, and ethoxzolamide. Incorporating different moieties into sulfonamides has proven to be a successful strategy for the researchers in their numerous attempts to create more potent and effective inhibitors [49,50]. Dithiocarbamate, selenide, chalcones, thiophenes, organotellurium compounds, 2-benzylpyrazine, and other new scaffolds were also developed as hCA II inhibitors, and their inhibitory ability was demonstrated in the nanomolar range. In vitro inhibitory effects of the target compounds **25–29** against hCA I and hCA II were assessed in comparison to commercially available hCA inhibitor acetazolamide as standard medication. Table 2 displays these drugs' anti-hCA actions (nM). The latter findings showed that most recently created drugs were more effective at inhibiting hCA I and hCA II than acetazolamide. It's interesting to note that the most active substances against the two tested enzymes were N,N-dimethyl-[3-(3,5-dimethoxyphenyl)propyl]sulfamide derivative **26** (hCA I), N,N-dimethyl-[3-(3,4-dimethoxyphenyl)propyl]sulfamide **27** (hCA II) and N,N-dimethyl-[3-(3,4-dimethoxyphenyl)propyl]sulfamide **28** (hCA II) were the less potent compounds (Figure 2).

Table 2. The inhibition results of the new sulfamide derivatives **25-29**
against hCA I and hCA II.

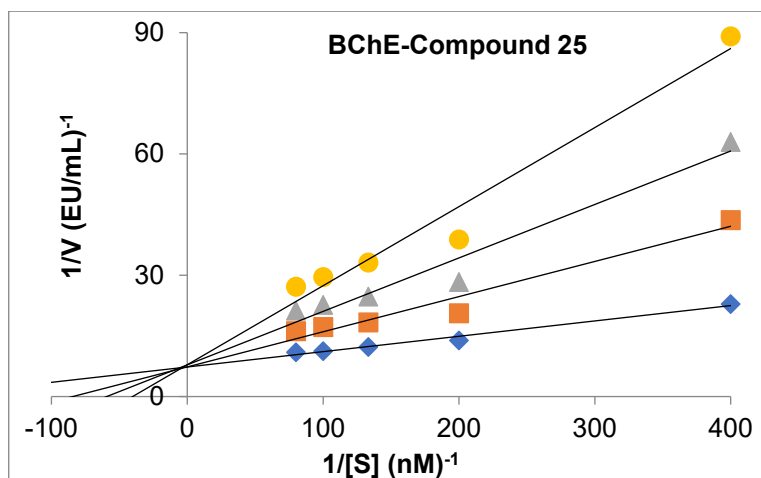| Compounds	IC_{50} (nM)				K_i (nM)	
	hCA I	r^2	hCA II	r^2	hCA I	hCA II
25	100.90	0.98	97.81	0.98	92.51±19.42	93.97±25.35
26	82.21	0.98	93.43	0.97	65.97±9.30	87.88±19.72
27	105.64	0.97	74.73	0.99	120.73±35.48	61.65±8.36
28	81.61	0.98	96.27	0.95	87.30±29.03	125.88±37.87
29	104.11	0.96	90.81	0.96	107.43±20.37	77.41±19.55
Acetazolamide	458.94	0.99	563.41	0.98	441.86±39.14	553.12±73.44
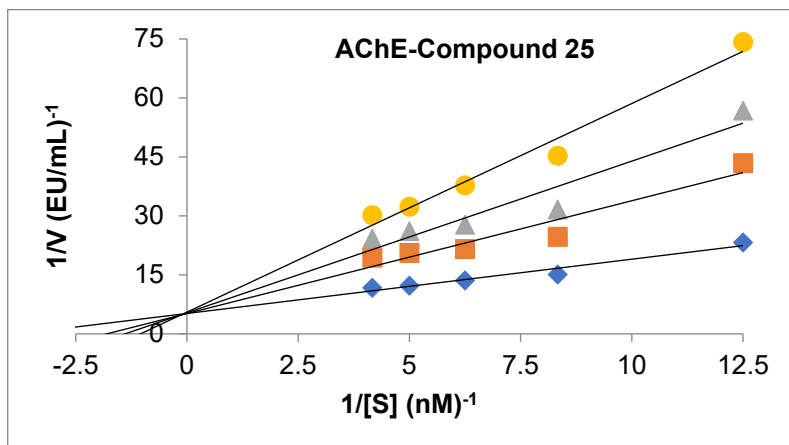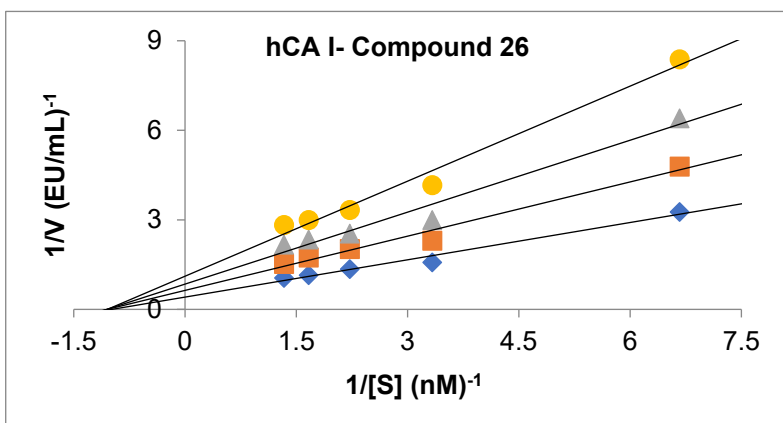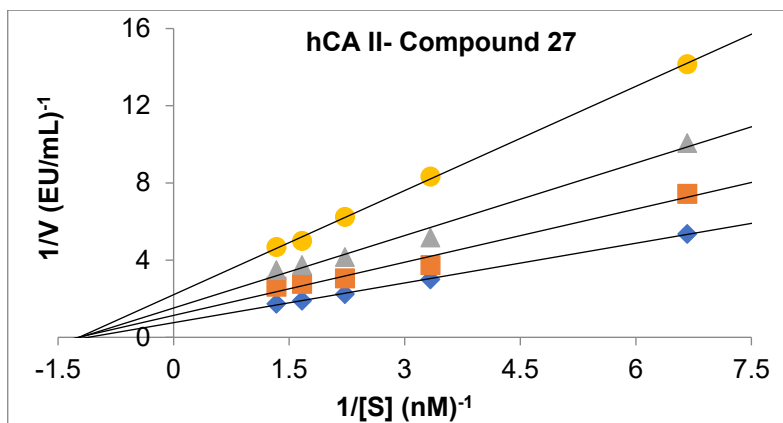
Figure 2. Lineweaver–Burk graphs of best inhibitors against human carbonic anhydrase I and II (hCA I and II), acetylcholinesterase (AChE) and butyrylcholinesterase (BChE) enzyme.

In silico studies

Binding site

SiteScore and Dscore were calculated to evaluate the receptor and co-crystal binding sites. Calculated SiteScore values for receptors AChE, BChE, hCA I and hCA II were 1.11, 1.16, 1.14, 1.00, respectively. In addition, the calculated Dscore values of these areas, which are considered as catalytic active sites, are examined in order to understand that they are druggable. Calculated Dscore values for receptors AChE, BChE, hCA I and hCA II were found 1.10, 1.21, 1.11, 0.83, respectively. When the values obtained as a result of Dscore and SiteScore calculations are examined, it has been determined that these regions may be catalytic active regions.

Molecular docking validation

Catalytic active sites determined receptors were prepared according to the IFD methodology. Co-crystals of the receptors were prepared for validation. In order to find the conformations between the receptor and ligands, a grid was created in co-crystal coordinates and the induced fit docking method was applied. The glide e-model value was also considered when

choosing the poses with the best binding affinities between the receptor and ligands. The glide e-model value gives the best pose information by eliminating inappropriate interactions between the conformations of the ligand, such as distant hydrogen bonds to the ligand. The glide e-model values for the receptor ligands 1YL, 3F9, 3TV and 51J are -77.78, -102.69, -65.50 and -108.56 (kcal/mol), respectively. The glide e-model values were confirmed the conformations of ligands that overlap with the co-crystals located at the catalytic active sites of the receptors. The docking verification results are shown in Figure 3. Contiguous positioning of the docking ligands with the co-crystals of the receptors confirmed the validation procedure.
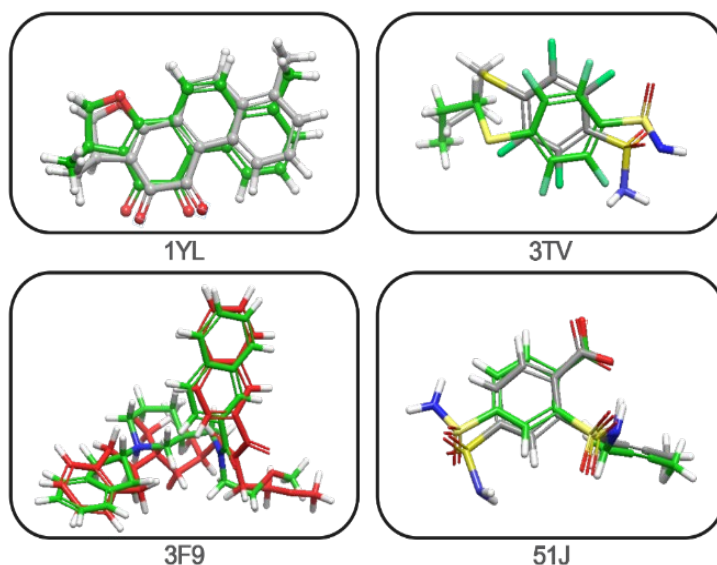

Figure 3. Docking methodology reliability test. The best-posed co-crystallized ligands are represented in green color ball and stick modelling and the best-posed docked ligands are represented in grey color ball and stick modelling for (1YL) AChE, (3F9) BChE, (3TV) hCA I, (51J) hCA II receptors.

Molecular docking and ADME studies

The rigid-receptor docking method, which is one of the methods used to calculate ligand-receptor interactions as *in-silico*, is useful when there are no significant changes in the binding surfaces between the protein and the ligand. However, this method is insufficient protein conformation that will

interact with ligands in the binding site [51]. For this reason, the induced fit docking method, which takes into account the ability of the ligand and the protein to adapt to each other and gives flexibility to the protein [52], was used in this study. The receptors X-Ray crystal structures for AChE (4M0E), BChE (4TPK), hCA I (4WR7), and hCA II (5AML) were used. These structures were chosen because they contain co-crystals in their catalytic active sites and have the appropriate resolution. In order to determine the interaction between the amino acids belonging to receptor and ligands, the poses with the greatest negative binding energies of the ligands in the binding pocket was chosen as the best position of the ligand.

The active site of the AChE (4M0E) receptor contains the ligand dihydrotanshinone (1YL-B:605) [53]. Dihydrotanshinone (1YL-B:605) is located in an area of approximately 10Å in diameter in the catalytic active site of amino acids S293, Y337, Y341 and W286. In addition, the 1YL ligand appears to interact with W286 by π-π stacking. All compounds were found to show high binding affinity when compared to the IFD score on the AChE binding pocket. The IFD scores for **25-29** compounds were found as -7.47, -6.92, -6.77, -6.38, and -6.95 kcal/mol, respectively (Table 3), and it seems to be compatible with the experimental data. In the AChE binding pocket, the compound with the highest IFD score was **25**. Compound **25** was showed interactions with amino acids within 4 Å in the AChE binding pocket and hydrophobic interactions, as seen in the 2D docking pose (Figure 4a). It is also seen that the compound **25** has a π-π stacking interaction with amino acid TYR341.

Table 3. IFD scores (kcal/mol) and Glide emodels (kcal/mol) of the compounds in the catalytic sites of AChE, BChE, hCA I, hCA II

Compounds	AChE		BChE		hCA I		hCA II	
	IFD Score	Glide emodel	IFD Score	Glide emodel	IFD Score	Glide emodel	IFD Score	Glide emodel
25	**-7.47**	**-59.92**	**-6.58**	**-56.71**	-5.93	-58.01	-6.63	-49.13
26	-6.92	-51.92	-6.35	-54.35	**-7.14**	**-63.26**	-6.98	-69.15
27	-6.77	-54.74	-5.77	-51.74	-6.17	-56.66	**-7.50**	**-75.96**
28	-6.38	-53.78	-6.06	-49.59	-6.63	-53.59	-6.59	-60.59
29	-6.95	-52.90	-5.30	-42.98	-6.48	-58.48	-6.18	-53.13

The BChE (4TPK) receptor binding site contains ligand N-((1-(2,3-dihydro-1H-inden-2-yl)piperidin-3-yl)methyl)-N-(2-methoxyethyl)-2-naphthamide (3F9-B:611). 3F9 ligand exhibits π-π stacking interaction with amino acids

ALI NADERI, AKIN AKINCIOĞLU, AHMET ÇAĞAN, SÜLEYMAN GÖKSU,
PARHAM TASLIMI, İLHAMI GÜLÇIN

F329 and W231 in this region of the receptor where amino acids Y332, I442, S72 and A328 are located. The calculated binding affinities between the BChE binding pocket and compounds **25-29** were -6.58, -6.35, -5.77, -6.06 and -5.30 kcal/mol, respectively. It is seen that these affinity values decreased in the order **25** > **26** > **28** > **27** > **29** (Table 3) and it is seen that this ranking coincides with the experimental data. From these affinity values, it is understood that the compound with the best IFD score in the BChE binding pocket is **25**, as in AChE. The 2D diagram of **25** shows hydrophobic interactions within 4 Å of its binding pocket. The interactions that affect the IFD score appear to be polar and hydrophobic interactions, in addition to the interactions between compound **25** and PHE 118 and LEU 286 amino acids in the active site of the BChE receptor (Figure 4b).
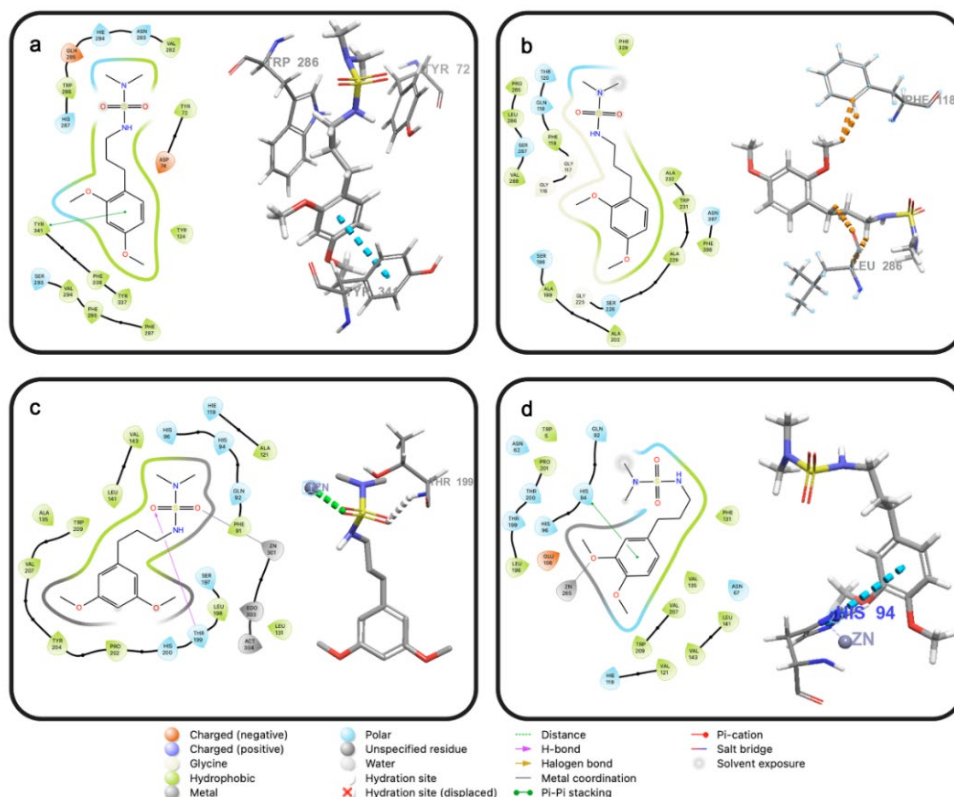

Figure 4. 2D and 3D ligand-receptor interaction profile of best-posed ligands into the receptors. (a) **25**-AChE, (b) **25**-BChE, (c) **26**-hCA I, (d) **27**-hCA II

The complex structure of hCA I (4WR7) includes 2,3,5,6-Tetrafluoro-4-(propylthio)benzenesulfonamide (3TV-B:302) ligand. In the catalytically active site where the 3TV ligand is located also has three histidine residues (H94, H96 and H119), and a zinc (B: ZN301) atom surrounded by a water molecule. In this region, amino acids A135, E106 and F91 are located, and there also appears to be a metal coordination bond between the amine group of 3TV and the zinc atom. The IFD score was calculated as -7.14 kcal/mol for **26**, which has the highest IFD score in the hCA I binding pocket. It can be thought that this value is the result of the hydrogen bond of one of the sulfamide oxygens in the structure of the compound **26** with THR 199 and the metal coordination bond of the other sulfamide oxygen with the zinc (ZN301) atom in the region (Figure 4c). It can be seen that there are interactions between the sulfamide group of the ligand 2-(but-2-yn-1-ylsulfamoyl)-4-sulfamoylbenzoic acid (51J-A:266) in the hCA II (5AML) complex and zinc (ZN265) in the catalytic active site of the protein. The IFD scores was calculated between the binding pocket in the catalytic active site of the hCA II receptor and compounds **25-29**. These values were found as -6.63, -6.98, -7.50, -6.59 and -6.18 kcal/mol, respectively. Compound **27** was showed the best affinity value for hCA II receptor. It can be deduced that this affinity value is the result of the π- π stacking interaction between **27** and HIS 94 in the binding pocket and the metal coordination between one of the methoxy groups and the zinc (ZN265) atom. (Figure 4d).

Table 4. ADME properties and drug similarity results of compounds

Compounds	MW mol[a]	Donor HB[b]	157ccept HB[c]	SASA[d]	Qplog[e] Po/w	Qplog BB[f]	QplogS[g]	% Human Oral Absorption[h]	Rule of Five[i]
25	302.39	1	4	550.15	3.24	-0.46	-3.40	100	0
26	302.39	1	4	577.63	3.21	-0.71	-3.89	100	0
27	302.39	1	4	559.64	3.25	-0.53	-3.57	100	0
28	272.36	1	3	523.45	3.03	-0.50	-3.35	100	0
29	242.34	1	3	513.59	3.11	-0.59	-3.58	100	0

[a]Moleculer Weight (acceptable range:<500). [b]Donor HB: Hyrogen bond donor (acceptable range: 0-5). [c]Accept HB: Hyrogen bond accetor (acceptable range: 0-5). [d]SASA:Total solvent accessible surface area using a probe with a 1.4 radius (acceptable range:300-1000). [e]Qplog Po/w Predicted octanol/water partition coefficient (–2.0 – 6.5). [f] Qplog BB Predicted Blood-brain partition coefficient (acceptable range:-2-1.2). [g]QplogS: Predicted aqueous solubility (–6.5 – 0.5). [h]% Human Oral Absorption: Predicted human oral absorption on 0 to 100% scale (<24% is poor and >80% is high). [i]Lipinski Rule of Five Violation

In this study, it was not only shown that the induced fit docking data were compatible with the experimental data but also the drug similarity studies of these compounds were conducted to evaluate the potential of the ligands to be a drug. For this purpose, the physicochemical properties known as Lipinski's rule of five were calculated *in silico.* These rules are used in drug design, predicting absorption and distribution in metabolism [54]. It is known that these rules should be considered in drug design [55]. In addition, drug-like compounds do not meet 2 or more of Lipinski's 5 rules will be problematic to distribute and absorb in the metabolism [56]. In light of this information, when Table 4 was examined, it was seen all of the compounds in our study were in accordance with Lipinski's rule of five.

CONCLUSION

In conclusion, novel sulfamides were synthesized starting from commercially available 4-phenylbutanoic acid derivatives. The hCA, AChE, and BChE inhibitory capacities of the produced compounds were assessed. The cytosolic isoforms hCA I and II were the targets of the compounds' CA inhibitory ability against the four physiologically relevant isoforms. All the chemicals effectively inhibited hCA I and II isozymes. The compounds were more potent and effective toward hCA II than hCA I, taking selectivity into account. The most effective compound was **27** with a Ki of 61.65 8.36 nM against hCA II, whereas compound **26** demonstrated effective inhibition with K_is of 65.97 9.30 nM for hCA I and II, respectively. Indeed, compounds **25**, **26**, and **29** may serve as lead compounds for the subsequent synthesis of powerful and specific cholinesterase inhibitors.

EXPERIMENTAL

All of the chemicals and solvents were utilized after distillation or after being treated with drying agents and are readily accessible on the market. The uncorrected melting points were found using a capillary melting device (BUCHI 530). Using a Perkin-Elmer spectrophotometer, IR spectra of solutions in 0.1 mm cells were obtained. The ^{1}H and ^{13}C NMR spectra were recorded on a 400 (100)-MHz Varian and 400 (100)-MHz Bruker spectrometer; d in ppm, Me$_4$Si as the internal standard. Elemental analyses were performed on a Leco CHNS-932 apparatus. All column chromatography was performed on silica gel (60-mesh, Merck). PLC is preparative thick-layer chromatography: 1 mm of silica gel 60 PF (Merck) on glass plates.

Synthesis

General synthetic procedure of carbamate derivatives

To a stirred solution of butanoic acid derivative in toluene (1 eq.) was added DPPA (1.2 eq) and NEt$_3$ (1.2 eq) at 25°C respectively. The reaction mixture was warmed to 110°C and magnetically stirred for 4h. Then, benzyl alcohol (4 eq) was added to the reaction mixture and stirred for 48 h at 110°C. After the reaction was controlled with TLC, the reaction solvent was evaporated under reduced pressure. The reaction mixture was purified with silica gel column chromatography with gradient solvent system (15%, 20%, 30% EtOAc\ Hexane). Compound **19** has been previously reported in the literature [57].

The synthesis of benzyl (3-(2,4 dimethoxyphenyl)propyl) carbamate (15)

Carbamate synthesis procedure described at **4.1.1** was applied to carboxylic acid **10** to give **15**. Colorless liquid, 83% yield. ^{1}H-NMR (400 MHz, CDCl$_3$, ppm): δ= 7.37-7.33 (m, 5H, Ar-H), 7.00 (d, 1H, Ar-H, J= 7.9 Hz), 6.42 (m, 1H, Ar-H), 6.40 (d, 1H, Ar-H, J= 2.2 Hz), 5.09 (s, 2H, CH$_2$), 4.89 (bs, 1H, NH), 3.785 (s, 3H, OCH$_3$), 3.781 (s, 3H, OCH$_3$), 3.20 (q, 2H, CH$_2$, J= 6.9 and J=13.0 Hz), 2.59 (t, 2H, CH$_2$, J= 7.3 Hz), 1.77 (p, 2H, CH$_2$, J= 6.9 and J=14.4 Hz). ^{13}C-NMR (100 MHz, CDCl$_3$, ppm): δ= 159.5 (C=O), 158.4 (C), 136.9(C), 130.3 (2CH), 128.7 (2CH), 128.3 (CH), 128.2 (CH), 127.2 (C), 122.3 (C), 104.2 (CH), 98.7 (CH), 66.7 (CH$_2$), 55.6 (OCH$_3$), 55.5 (OCH$_3$), 40.7 (CH$_2$), 30.5 (CH$_2$), 26.7 (CH$_2$). IR (CH$_2$Cl$_2$, cm^{-1}): 3340, 2931, 1707, 1612, 1587, 1507, 1454, 1289, 1258, 1208, 1155, 1132, 1037. Anal. Calcd for (C$_{19}$H$_{23}$NO$_4$); C, 69.28; H, 7.04; N, 4.25; Found C, 69.30; H, 7.00; N, 4.28.

The synthesis of benzyl (3-(3,5-dimethoxyphenyl)propyl)carbamate (16)

The procedure described at 4.1.1 was applied to carboxylic acid **11** to give **16**. White solid, 85% yield. Mp: 54-56 °C. ^{1}H-NMR (400 MHz, CDCl$_3$, ppm): δ= 7.37-7.34 (m, 5H, Ar-H), 6.34 (m, 2H, Ar-H), 6.31 (d, 1H, Ar-H, J= 1.8 Hz), 5.09 (s, 2H, CH$_2$), 4.30 (bs, 1H, NH), 3.77 (s, 3H, OCH$_3$), 3.75 (s, 3H, OCH$_3$), 3.22 (q, 2H, CH$_2$, J= 6.6 and J=13.0 Hz), 2.59 (t, 2H, CH$_2$, J= 7.6 Hz), 1.80 (p, 2H, CH$_2$, J= 6.6 and J=14.2 Hz). ^{13}C-NMR (100 MHz, CDCl$_3$, ppm): δ= 161.0 (C=O), 144.0 (2C), 141.2 (C), 136.8 (C), 128.7 (2CH), 128.3 (2CH), 106.6 (2CH), 98.1 (2CH), 66.9 (CH$_2$), 55.5 (2OCH$_3$), 40.9 (CH$_2$), 33.6 (CH$_2$), 31.6 (CH$_2$). IR (CH$_2$Cl$_2$, cm^{-1}): 3338, 2937, 2840, 1703, 1596, 1530, 1456, 1243, 1205, 1150, 1058. Anal. Calcd for (C$_{19}$H$_{23}$NO$_4$); C, 69.28; H, 7.04; N, 4.25; Found C, 69.25; H, 7.02; N, 4.26.

The synthesis of benzyl (3-(3,4-dimethoxyphenyl)propyl)carbamate (17)

The procedure described at **4.1.1** was applied to carboxylic acid **12** to give **17**. White solid, 82% yield. Mp: 63-65 °C. ^{1}H-NMR (400 MHz, CDCl$_3$, ppm): δ= 7.35-7.28 (m, 5H, Ar-H), 6.77 (d, 1H, Ar-H, J= 7.6 Hz), 6.69 (d, 2H, Ar-H, J= 7.6 Hz), 5.09 (s, 2H, CH$_2$), 4.87 (bs, 1H, NH), 3.84 (s, 3H, OCH$_3$), 3.83 (s, 3H, OCH$_3$), 3.21 (q, 2H, CH$_2$, J= 6.9 and J=13.2 Hz), 2.58 (t, 2H, CH$_2$, J= 7.3 Hz), 1.80 (p, 2H, CH$_2$, J= 6.9 and J=14.5 Hz). ^{13}C-NMR (100 MHz, CDCl$_3$, ppm): δ= 156.7 (C=O), 149.1 (C), 147.5 (C), 136.8 (C), 134.2 (C), 128.7 (CH), 128.3 (CH), 120.4 (CH), 111.9 (CH), 111.5 (2CH), 66.8 (CH$_2$), 56.1 (OCH$_3$), 56.0 (OCH$_3$), 40.8 (CH$_2$), 32.8 (CH$_2$), 31.9 (CH$_2$). IR (CH$_2$Cl$_2$, cm[-1]): 3365, 3036, 2935, 2857, 1704, 1590, 1515, 1454, 1259, 1140, 1028. Anal. Calcd for (C$_{19}$H$_{23}$NO$_4$); C, 69.28; H, 7.04; N, 4.25; Found C, 69.26; H, 7.01; N, 4.22.

The synthesis of benzyl (3-(4-metoxyphenyl)propyl)carbamate (18)

Carbamate procedure described at **4.1.1** was applied to carboxylic acid **13** to give **18**. White solid, 83% yield. Mp: 48-50 °C. ^{1}H-NMR (400 MHz, CDCl$_3$, ppm): δ= 7.36-7.30 (m, 5H, Ar-H), 7.09 (d, 2H, Ar-H, J= 8.2 Hz), 6.83 (d, 2H, Ar-H, J= 8.2 Hz), 5.10 (s, 2H, CH$_2$), 4.84 (bs, 1H, NH), 3.78 (s, 6H, 2OCH$_3$), 3.22 (q, 2H, CH$_2$, J= 6.8 and J=13.2 Hz), 2.59 (t, 2H, CH$_2$, J= 7.7 Hz), 1.80 (p, 2H, CH$_2$, J= 6.8 and J=14.4 Hz). ^{13}C-NMR (100 MHz, CDCl$_3$, ppm): δ= 158.1 (C=O), 156.7 (C), 136.9 (C), 133.7 (C), 129.5 (3CH), 128.8 (2CH), 128.3 (CH), 114.1 (3CH), 66.8 (CH$_2$), 55.5 (OCH$_3$), 40.8 (CH$_2$), 32.3 (CH$_2$), 32.0 (CH$_2$). IR (CH$_2$Cl$_2$, cm[-1]): 3334, 3030, 2935, 2857, 1698, 1612, 1512, 1454, 1245, 1177, 1134, 1034. Anal. Calcd for (C$_{18}$H$_{21}$NO$_3$); C, 72.22; H, 7.07; N, 4.68; Found C, 72.25; H, 7.04; N, 4.66.

The general hydrogenolysis procedure for the synthesis of amine hydrochloride salt derivatives from carbamates

Pd/C (10%) and CHCl$_3$ (2 mL) were added to a stirred solution of the carbamate (5 mmol) in MeOH (40 mL). The reaction flask was three times discharged and inflated with H$_2$ (in the basic party balloon). Then, the reaction mixture was magnetically stirred at 25°C for 12 h. The reaction solvent was leached through grade 4 filter paper. Then leachate was evaporated, and the amine salt was purified from the reaction residue by crystallization in the MeOH-Et$_2$O solvent system. The synthesis of amine derivatives **22-24** have been previously reported in the literature [58-60].

The synthesis of 3-(2,4-dimethoxyphenyl)propan-1-amine hydrochloride (20)

Amine salt **20** was synthesized from **15** as described above. White solid, 79% yield. Mp: 178-180 °C. ^{1}H-NMR (400 MHz, D$_2$O, ppm): δ= 7.03 (d, 1H, Ar-H, J= 8.3 Hz), 6.51 (d, 1H, Ar-H, J= 2.3 Hz), 6.47 (dd, 1H, Ar-H, J= 2.5 and J= 8.3 Hz), 3.71 (s, 3H, OCH$_3$), 3.69 (s, 3H, OCH$_3$), 2.84 (t, 2H, CH$_2$, J= 7.4 Hz), 2.52 (t, 2H, CH$_2$, J= 7.4 Hz), 1.79 (p, 2H, CH$_2$, J= 7.4 and J=15 Hz). ^{13}C-NMR

(100 MHz, D_2O, ppm): δ= 159.0 (C), 158.2 (C), 130.8 (CH), 121.8 (C), 105.6 (CH), 99.1 (CH), 55.7 (2OCH$_3$), 39.1 (CH$_2$), 27.5 (CH$_2$), 25.6 (CH$_2$).

The synthesis of 3-(2,4-dimethoxyphenyl)propan-1-amine hydrochloride (21):

Amine salt **21** was synthesized from **16** as in described synthesis procedure **4.2**. White solid, 82% yield. Mp: 150-152 °C. ^{1}H-NMR (400 MHz, D_2O, ppm): δ= 6.38 (d, 1H, Ar-H, J= 2.2 Hz), 6.31- 6.30 (m, 2H, Ar-H), 3.642 (s, 3H, OCH$_3$), 3.648 (s, 3H, OCH$_3$), 2.84 (t, 2H, CH$_2$, J= 7.7 Hz), 2.53 (t, 2H, CH$_2$, J= 7.6 Hz), 1.83 (p, 2H, CH$_2$, J= 7.6 and J=15.4 Hz). ^{13}C-NMR (100 MHz, D_2O, ppm): δ= 160.5 (2C), 143.9 (C), 107.1 (2CH), 98.3 (CH), 55.6 (2OCH$_3$), 39.1 (CH$_2$), 32.1 (CH$_2$), 28.3 (CH$_2$).

General procedure for the synthesis of sulfamide derivatives from amine hydrochloride salts:

To a stirred solution of amine hydrochloride salt (1 eq) in CH_2Cl_2 (30 mL) was added NEt$_3$ (2.5 eq) at rt and the reaction mixture was magnetically stirred at rt for 3 h. Then, the reaction mixture was cooled to 0°C and N, N-dimethylsulfamoyl chloride (1.1 eq) was added to the reaction mixture under N$_2$ atm. The reaction mixture was warm to rt and magnetically stirred for 24 h. H$_2$O was added to the reaction mixture and pH was adjusted to 6 with 0.1 M HCl. The organic phase was separated and the water phase was extracted two times with CH_2Cl_2 (30 mL). The combined organic phases were dried over Na$_2$SO$_4$. The solvent was evaporated under reduced pressure. The residue was purified by silica gel column chromatography with EtOAc-Hexane (1:4) solvent system.

N,N-dimethyl-[3-(2,4-dimethoxyphenyl)propyl] sulfamide (25)

The general sulfamide synthesis described in **4.3** was applied to amine hydrochloride salt derivative **20** to yield sulfamide derivative **25**. Viscous liquid, 8**0**% yield. ^{1}H-NMR (400 MHz, CDCl$_3$, ppm): δ= 7.00 (d, 1H, Ar-H, J= 8.0 Hz), 6.43 (dd, 2H, Ar-H, J= 2.4 and J= 10.8 Hz), 4.38 (t, 1H, NH, J= 5.4 Hz), 3.80 (s, 3H, OCH$_3$), 3.78 (s, 3H, OCH$_3$), 3.02 (q, 2H, CH$_2$, J= 6.7 and J= 13.1 Hz), 2.78 (s, 6H, 2CH$_3$), 2.60 (t, 2H, CH$_2$, J= 7.4 Hz), 1.78 (p, 2H, CH$_2$, J= 6.7 and J=14.1 Hz). ^{13}C-NMR (100 MHz, CDCl$_3$, ppm): δ= 159.6 (C), 130.5 (CH), 121.7 (C), 111.6 (C), 104.4 (CH), 98.8 (CH), 55.6 (OCH$_3$), 55.5 (OCH$_3$), 43.0 (CH$_2$), 38.3 (2CH$_3$), 30.5 (CH$_2$), 26.4 (CH$_2$). IR (CH$_2$Cl$_2$, cm^{-1}): 3301, 2997, 2938, 2838, 1612, 1588, 1508, 1459, 1439, 1419, 1324, 1291, 1261, 1208, 1179, 1153, 1084, 1043. Anal. Calcd for (C$_{13}$H$_{22}$N$_2$O$_4$S); C, 51.64; H, 7.33; N, 9.26; S, 10.60; Found C, 51.60; H, 7.35; N, 9.28; S, 10.63.

N,N-dimethyl-[3-(3,5-dimethoxyphenyl)propyl] sulfamide (26)

The procedure described in **4.3** was applied to amine hydrochloride salt **21** to yield sulfamide **26**. Viscous liquid, 77% yield. ^{1}H-NMR (400 MHz, CDCl$_3$, ppm): δ= 6.33 (d, 2H, Ar-H, J= 2.2 Hz), 6.30 (d, 1H, Ar-H, J= 2.2 Hz), 4.48 (t, 1H, NH, J= 5.5 Hz), 3.76 (s, 6H, 2OCH$_3$), 3.05 (q, 2H, CH$_2$, J= 7.0 and J= 13.6 Hz), 2.77 (s, 6H, 2CH$_3$), 2.60 (t, 2H, CH$_2$, J= 7.5 Hz), 1.85 (p, 2H, CH$_2$, J= 7.0 and J=16 Hz). ^{13}C-NMR (100 MHz, CDCl$_3$, ppm): δ= 161.1 (2C), 143.6 (C), 106.7 (CH), 98.2 (CH), 55.5 (2OCH$_3$), 43.2 (CH$_2$), 38.2 (2CH$_3$), 33.3 (CH$_2$), 31.4 (CH$_2$). IR (CH$_2$Cl$_2$, cm^{-1}): 3300, 2940, 2840, 1596, 1460, 1429, 1324, 1259, 1205, 1149, 1055. Anal. Calcd for (C$_{13}$H$_{22}$N$_2$O$_4$S); C, 51.64; H, 7.33; N, 9.26; S, 10.60; Found C, 51.66; H, 7.35; N, 9.29; S, 10.63.

N,N-dimethyl-[3-(3,4-dimethoxyphenyl)propyl] sulfamide (27)

The procedure described in **4.3** was applied to amine hydrochloride salt **22** to yield sulfamide **27**. White solid, 80% yield. Mp: 100-102 °C. ^{1}H-NMR (400 MHz, CDCl$_3$, ppm): δ= 6.78 (d, 1H, Ar-H, J= 8.5 Hz), 6.70 (d, 1H, Ar-H, J= 2.2 Hz), 4.37 (t, 1H, NH, J= 5.8 Hz), 3.86 (s, 3H, OCH$_3$), 3.84 (s, 3H, OCH$_3$), 3.06 (q, 2H, CH$_2$, J= 6.9 and J= 13.8 Hz), 2.78 (s, 6H, 2CH$_3$), 2.61 (t, 2H, CH$_2$, J= 7.7 Hz), 1.84 (p, 2H, CH$_2$, J= 6.9 and J=14.6 Hz). ^{13}C-NMR (100 MHz, CDCl$_3$, ppm): δ= 149.1 (C), 147.6 (C), 133.8 (C), 120.4 (CH), 111.9 (CH), 111.5 (CH), 56.1 (OCH$_3$), 56.08 (OCH$_3$), 43.2 (CH$_2$), 38.3 (2CH$_3$), 32.6 (CH$_2$), 31.8 (CH$_2$). IR (CH$_2$Cl$_2$, cm^{-1}): 3295, 2937, 2840, 1591, 1516, 1463, 1419, 1325, 1260, 1235, 1144, 1083, 1027. Anal. Calcd for (C$_{13}$H$_{22}$N$_2$O$_4$S); C, 51.64; H, 7.33; N, 9.26; S, 10.60; Found C, 51.65; H, 7.30; N, 9.28; S, 10.65.

N,N-dimethyl-[3-(3,4-dimethoxyphenyl)propyl]sulfamide (28)

The procedure described in **4.3** was applied to amine hydrochloride salt **23** to produce sulfamide **28**. White solid, 77% yield. Mp: 82-84 °C. ^{1}H-NMR (400 MHz, CDCl$_3$, ppm): δ= 7.08 (d, 2H, Ar-H, J= 8.4 Hz), 6.81 (d, 2H, Ar-H, J= 8.4 Hz), 4.47 (t, 1H, NH, J= 5.7 Hz), 3.77 (s, 3H, OCH$_3$), 3.05 (q, 2H, CH$_2$, J= 7.3 and J= 13.4 Hz), 2.778 (s, 3H, CH$_3$), 2.775 (s, 3H, CH$_3$), 2.61 (t, 2H, CH$_2$, J= 7.3 Hz), 1.84 (p, 2H, CH$_2$, J= 7.3 and J=14.4 Hz). ^{13}C-NMR (100 MHz, CDCl$_3$, ppm): δ= 158.1 (C), 133.3 (C), 129.5 (2CH), 114.1 (2CH), 55.50 (OCH$_3$), 55.48 (OCH$_3$), 43.2 (CH$_2$), 38.2 (2CH$_3$), 32.2 (CH$_2$), 31.9 (CH$_2$). IR (CH$_2$Cl$_2$, cm^{-1}): 3283, 2957, 2931, 2857, 1610, 1514, 1457, 1436, 1326, 1255, 1240, 1150, 1077, 1029. Anal. Calcd for (C$_{12}$H$_{20}$N$_2$O$_3$S); C, 52.92; H, 7.40; N, 10.29; S, 11.77; Found C, 52.90; H, 7.44; N, 10.31; S, 11.75.

N,N-dimethyl-[3-(phenyl)propyl]sulfamide (29)

The general procedure described in **4.3** was applied to amine hydrochloride salt **24** to yield sulfamide **29**. Viscous liquid, 74% yield. ^{1}H-NMR (400 MHz, Acetone-d$_6$, ppm): δ= 7.35-7.26 (m, 3H, Ar-H), 7.21-7.17 (m, 2H, Ar-H), 4.41

(bs, 1H, NH), 3.09 (q, 2H, CH$_2$, J= 6.9 and J= 12 Hz), 2.78 (s, 6H, 2CH$_3$), 2.69 (t, 2H, CH$_2$, J= 7.6 Hz), 1.90 (p, 2H, CH$_2$, J= 6.9 and J=14.8 Hz). ^{13}C-NMR (100 MHz, Acetone-d$_6$, ppm): δ= 141.2 (C), 128.7 (2CH), 128.6 (2CH), 126.3 (CH), 43.3 (CH$_2$), 38.2 (2CH$_3$), 33.1 (CH$_2$), 31.7 (CH$_2$). IR (CH$_2$Cl$_2$, cm^{-1}): 3297, 3026, 2938, 2879, 1702, 1602, 1496, 1454, 1324, 1255, 1148, 1084, 1055. Anal. Calcd for (C$_{11}$H$_{18}$N$_2$O$_2$S); C, 54.52; H, 7.49; N, 11.56; S, 13.23; Found C, 54.55; H, 7.53; N, 11.58; S, 13.20.

hCA isoenzyme purification and inhibition studies

CA isoforms from human erythrocytes were purified in one step using the Sepharose-4B-L-Tyrosine-sulphanilamide affinity gel chromatography method in order to investigate the inhibitory effects of the new sulfamide derivatives **25-29** on hCA I and II. The target compounds were then evaluated in accordance with the literature [61,62]. The Bradford method, which has been used in other investigations, was used to assess the amount of protein present during the purification phases [63]. As a benchmark, bovine serum albumin protein was used. SDS-PAGE was used to monitor the purity of both hCA isoforms, as previously reported in research. Esterase activity was assessed during the inhibition and purification of both hCA isoforms. The activity of both hCA isoforms was assessed by monitoring the shift in 348 nm absorbance. The enzyme activity (%) versus inhibitor plots were used to determine the IC$_{50}$ and K$_i$ parameters. We calculated the Ki values and other inhibition factors using Lineweaver-Burk graphs [64].

Cholinesterases assays

The Ellman's method [45] method was used to test the inhibition effects of new sulfamide derivatives **25-29** on AChE/BChE activity as described previously [65,66]. The AChE/BChE activities were measured using DTNB (Product No. D8130-1G, Sigma-Aldrich) and AChI/BChI. Specifically, 10 µL of the sample solution were dissolved in 100 µL of buffer (Tris/HCl, 1 M, pH 8.0), with various concentrations of the sample solution. AChE/BChE solution was then added, and 50 µL was incubated at 25 °C for 10 minutes. A quantity of DTNB (50 µL, 0.5 mM) was added following incubation. Finally, 50 µL of AChI/BChI were added to the reaction to begin it (10 mM, Product no: 01480-1G, Sigma-Aldrich). By observing the spectrophotometric production of the yellow 5-thio-2-nitrobenzoate anion as a result of the reaction of DTNB with thiocholine at a wavelength of 412 nm, it was possible to quantify the enzymatic hydrolysis of both substrates. Different amounts of new sulfamide derivatives **25-29** were added to the

reaction mixture in order to determine their impact on AChE. Following that, AChE/BChE activity were assessed. The plots of activity (%) vs compounds were used to get the IC_{50} values.

Binding site prediction

Ligand binding sites predicted as the catalytic active sites of the receptors were evaluated. For this purpose, SiteScore and Dscore values were calculated using Maestro 13.4.134 [67] SiteMap tool [68]. This process provides information about the catalytically active sites that will be used for all ligands and it gives information about the druggable of these areas [69].

Protein preparation

X-Ray structures of the receptors to be used in the docking study to be carried out in accordance with the IFD methodology, AChE, BChE, hCA I, hCA II (PDB code: 4M0E, 4TPK, 4WR7, and 5AML, respectively) were obtained from the RCSB Protein Data Bank (PDB; http://www. rcsb.org/). Receptors were repaired and prepared using the Protein Preparation [70] tool. The simulation was carried out at physiological pH 7.4 and under these conditions, the missing amino acids in the receptor were added. The errors of the receptors were checked at this stage. After it was understood that the errors were corrected, the conformations of the hydrogens were arranged and the charge was determined. The energies of the receptors were minimized using force filed OPLS_2005 [71] and their geometry was optimized.

Ligand preparation

Two-dimensional structures of all ligands were drawn with ChemDraw 15.1.0.144 and three-dimensional structures were obtained with Maestro 13.4.134. All ligands were ionized at pH 7.0 ± 2 using the Maestro 13.4.134 LigPrep [72] tool and all possible structures were obtained by bringing them to the correct molecular geometry and protonation state.

Induce Fit Docking

Maestro 13.4.134 InduceFitDocking [73] tool was used to characterize the interactions and binding affinity between the receptors prepared during the validation process, determined catalytic active sites and ligands prepared according to the IFD methodology. The catalytically active sites were gridded and the residues closest to the ligand were corrected for those within 5.0 Å of the ligand pose. The best IFD scores of the components are given in Table 3.

ADME Study

Drug likeness was evaluated by conducting an ADME study of the compounds. For this purpose, the two-dimensional structures of the compounds were drawn with ChemDraw 15.1.0.144 and the molecular weights, hydrogen acceptor and donor bond numbers, solvent surface access area, octanol/water distribution coefficient, estimated blood-brain, predicted water solubility, human oral absorption and Lipinski rule violations were calculated with Maestro 13.4.134 QikProb [74] tool.

ACKNOWLEDGMENTS

REFERENCES

1. Jun, J. J.; Xie, X.Q. *ChemistrySelect*. **2021**, *6*, 430–469.
2. Jun, J. J.; Duscharla, D.; Ummanni, R.; Hanson, P. R.; Malhotra, S. V. *Med. Chem. Lett.* **2021**, *12*, 202−210.
3. Backbro, K.; Löwgren, S.; Österlund, K.; Atepo, J.; Unge, T.; Hulten, J.; Bonham, N. M.; Schaal, W.; Karle´n, A.; Hallberg, A. *J. Med. Chem.* **1997**, *40* (6), 898−902.
4. Dow, R.L.; Paight, E.S.; Schneider, S.R.; Hadcock, J.R.; Hargrove, D.M.; Martin, K.A.; Maurer, T.S.; Nardone, N.A.; Tess, D.A.; DaSilva-Jardine, P. *Bioorg. Med. Chem. Lett.* **2004**, *14*, 3235–3240.
5. Hulten, J.; Bonham, N. M.; Nillroth, U.; Hansson, T.; Zuccarello, G.; Bouzide, A.; Åqvist, J.; Classon, B.; Danielson, U. H.; Karlen, A. *J. Med. Chem.* **1997**, *40*, 885−897.
6. Hirayama, F.; Koshio, H.; Katayama, N.; Ishihara, T.; Kaizawa, H.; Taniuchi, Y.; Sato, K.; Sakai-Moritani, Y.; Kaku, S.; Kurihara, H.; Kawasaki, T.; Matsumoto, Y.; Sakamoto, S.; Tsukamoto, S. *Bioorg. Med. Chem.* **2003**, *11*, 367−381.
7. Dou, D. F.; Tiew, K. C.; He, G. J.; Mandadapu, S. R.; Aravapalli, S.; Alliston, K. R.; Kim, Y.; Chang, K. O.; Groutas, W. C. *Bioorg. Med. Chem.* **2011**, *19*, 5975−5983.
8. Abbaz, T.; Bendjeddou, A.; Gouasmia, A.; Bouchouk, D.; Boualleg, C.; Kaouachi, N.; Inguimbert, N.; Villemin, D. *Lett. Org. Chem.* **2014**, *11*, 59-63.
9. Groutas, W. C.; Schechter, N. M.; He, S.; Yu, H.; Huang, P.; Tu, J. *Bioorg. Med. Chem. Lett.* **1999**, *9*, 2199–2204.
10. Lee, K.; Park, C. W.; Jung, W. H.; Park, H. D.; Lee, S. H.; Chung, K. H.; Park, S. K.; Kwon, O. H.; Kang, M.; Park, D.-H. *J. Med. Chem*. **2003**, *46*, 3612–3622.
11. Winum, J.Y.; Scozzafava, A.; Montero, J.L.; Supuran, C.T. *Med. Res. Rev*. **2006**, 26, 767-792.

12. Langtry, H.D.; Grant, S. M.; Goa K. L. *Drugs* **1989**, *38* (4): 551-590.

13. Barlier, A.; Jaquet, P. *Eur. J. Endocrinol.* **2006**, *154*, 187–195. DOI: 10.1530/eje.1.02075

14. Hong, I.S.; Coe, H.V.; Catanzaro. L.M. *Ann. Pharmacother.* **2014**, *48* (4): 538–547.

15. Mazzei, T. *J Chemotherapy* **2010**, 22, 219-225.

16. Akıncıoğlu, A.; Kocaman, E.; Akıncıoğlu, H.; Salmas, R. E.; Durdagi, S.; Gülçin, İ.; Supuran, C. T.; Göksu, S. *Bioorg. Chem.* **2017**, *74*, 238-250.

17. Akıncıoğlu, A.; Göksu, S.; Naderi, A.; Akıncıoğlu, H.; Kılınç, N.; Gülçin, İ. *Computational Biology and Chemistry* **2021**, *94*, 107565.

18. Göksu, S.; Naderi, A.; Akbaba, Y.; Kalın, P.; Akıncıoğlu, A.; Gülçin, İ.; Durdagi, S.; Salmas, R. E. *Bioorg Chem.* **2014**, *56*, 75-82.

19. Akıncıoğlu, A.; Akıncıoğlu, H.; Gülçin, İ.; Durdagi, S.; Supuran, C. T.; Göksu, S. *Bioorganic & Medicinal Chemistry* **2015**, *23*(13), 3592-3602.

20. Aksu, K.; Akıncıoğlu, H.; Akıncıoğlu, A.; Göksu, S.; Tumer, F.; Gulcin, I. *Archiv der Pharmazie* **2018**, *351*, 1800150.

21. Aksu, K.; Nar, M.; Tanç, M.; Vullo, D.; Gülçin, I.; Göksu, S.; Tümer, F.; Supuran, C. T. *Bioorg Med Chem* **2013**, *21*, 2925-31.

22. Akıncıoğlu, A.; Akbaba, Y.; Göçer, H.; Göksu, S.; Gülçin, İ.; Supuran, C. T. *Bioorg. Med. Chem.* **2013**, *21*, 1379-1385.

23. Özgeriş, B.; Göksu, S.; Köse, L. P.; Gülçin, I.; Salmas, R. E.; Durdagi, S.; Tümer, F.; Supuran, C. T. *Bioorg. Med. Chem.* **2016**, *24*, 2318-2329.

24. Taslimi, P.; Gulcin, I.; Ozgeris, B.; Goksu, S.; Tumer, F.; Alwasel, S. H.; Supuran, C. T. *J. Enzyme Inhib. Med. Chem.,* **2016**, *31*, 152-157.

25. Akıncıoğlu, A.; Topal, M.; Gülçin, I.; Göksu, S. *Arch. der Pharm.* **2014**: *347*, 68-76.

26. Göksu, S.; Kazaz, C.; Sütbeyaz, Y.; Secen, H. *Helv. Chim. Acta* **2003**, *86*, 3310-3313.

27. Akbaba, Y.; Akıncıoğlu, A.; Göçer, H.; Göksu, S.; Gülçin, İ.; Supuran, C.T. *J. Enzyme Inhib. Med. Chem.* **2014**, *29* (1), 35-42.

28. Biçer, A.; Taslimi, P.; Yakali, G.; Gülçin, İ.; Gültekin, M.S.; Turgut Cin, G. *Bioorg. Chem.* **2019**, *82*, 393-404.

29. Huseyinova, A.; Kaya, R.; Taslimi, P.; Farzaliyev, V.; Mammadyarova, X.; Sujayev, A.; Tüzün, B.; Türkan, F.; Koçyiğit, U.M.; Alwasel, S.; Gulcin, İ. *J. Biomol. Struct. Dyn.* **2021**, *40*(1), 236-248.

30. Hashmi, S.; Khan, S.; Shafiq, Z.; Taslimi, P.; Ishaq, M.; Sadeghian, N.; Karaman, S.H.; Akhtar, N.; Islam, M.; Asari, A.; Mohamad, H.; Gulcin, İ. *Bioorg. Chem.* **2021**, *107*, 104554.

31. Cabaleiro-Lago, C.; Lundqvist, M. *Molecules*. **2020**, *25*, 4405.

32. Çelebioglu, H.U.; Erden, Y.; Hamurcu, F.; Taslimi, P.; Şentürk, O.Ş.; Özdemir Özmen, Ü.; Tüzün, B.; Gulcin, İ. *J. Biomol. Struct. Dyn.* **2021**, *39*, 5539-5550. DOI: 10.1080/07391102.2020.1792345

33. Taslimi, P.; Akıncıoğlu, H.; Gulçin, İ. *J. Biochem. Mol. Toxicol.* **2017**, *31*(11), e21973. DOI: 10.1002/jbt.21973

34. Çetin Çakmak, K.; Gülçin, İ. *Toxicol. Rep.* **2019**, *6*, 1273-1280.

35. Pedrood, K.; Sherefati, M.; Taslimi, P.; Mohammadi-Khanaposhtani, M.; Asgari, M.S.; Hosseini, S.; Rastegar, H.; Larijani, B.; Mahdavi, M.; Taslimi, P.; Erden, Y.; Günay, S.; Gulçin, İ. *Int. J. Biol. Macromol.* **2021**, *170*, 1-12.

36. Taslimi, P.; Koksal, E.; Gören, A.C.; Bursal, E.; Aras, A.; Kılıç, O.; Alwasel, S.; Gulçin, İ. *Arab. J. Chem.* **2020**, *13*(3), 4528-4537.

37. Sepheri, N.; Mohammadi-Khanaposhtani, M.; Asemanipoor, N.; Hosseini, S.; Biglar, M.; Larijani, B.; Mahdavi, M.; Hamedifar, H.; Taslimi, P.; Sadeghian, N.; Gulçin, İ. *Arch. Pharm.* **2020**, 353(10), e2000109.

38. Öztaskın, N.; Göksu, S.; Demir, Y.; Maraş, A.; Gulçin, İ. *Molecules* **2022**, *27*(21), 7426.

39. Ghosh, A. K.; Sarkar, A.; Brindisi, M. *Org. Biomol. Chem.* **2018**, *16*, 2006-2027.

40. Öztaşkın, N.; Göksu, S.; Secen, H. *Synthetic Commun.* **2011**, *41*, 2017-2024.

41. Güzel, E.; Koçyiğit, U.M.; Taslimi, P.; Gulçin, İ.; Erkan, S.; Nebioğlu, M.; Aslan, B.S.; Şişman, İ. *J. Biomol. Struct. Dyn.* **2022**, *40*, 733-741.

42. Aktas, A.; Barut Celepci, D.; Gök, Y.; Taslimi, P.; Akıncıoğlu, H.; Gülçin, İ. *Crystals* **2020**, *10*, 171.

43. Ozmen Ozgün, D.; Gül, H.İ.; Yamali, C.; Sakagami, H.; Gulçin, İ.; Sukuroglu, M.; Supuran, C.T. *Bioorg. Chem.* **2019**, *84*, 511-517.

44. Karimov, A.; Orujova, A.; Taslimi, P.; Sadeghian, N.; Mammadov, B.; Karaman, H.S.; Farzaliyev, V.; Sujayev, E.; Taş, R.; Alwasel, S.; Gulçin, İ. *Bioorg. Chem.* **2020**, 99, 103762.

45. Ellman, G.L.; Courtney, K.D.; Andre,s V.; Feather-Stone, R.M. *Biochem. Pharmacol.* **1961**, *7*, 88–95.

46. Sujayev, A.; Garibov, E.; Taslimi, P.; Gülçin, İ.; Gojayeva, S.; Farzaliyev, V.; Alwasel, S.H.; Supuran, C.T. *J. Enzyme Inhib. Med. Chem.* **2016**, *31*(6), 1531-1539.

47. Bayrak, Ç.; Taslimi, P.; Gülçin, İ.; Menzek, A. *Bioorg. Chem.* **2017**, *72*, 359-366.

48. Taslimi, P.; Caglayan, C.; Gulçin, İ. *J. Biochem. Mol. Toxicol.* **2017**, *31*(12), e21995.

49. Koçyigit, M.U.; Taslimi, P.; Gurses, F.; Soylu, S.; Durna Dastan, S.; Gulçin, İ. *J. Biochem. Mol. Toxicol.* **2018**, *32*(3), e22031.

50. Turkan, F.; Huyut, Z.; Taslimi, P.; Gulçin, İ. *J. Biochem. Mol. Toxicol.* **2018**, *32*(3), e22041.

51. Sherman, W.; Day, T.; Jacobson, M. P.; Friesner, R. A.; Farid, R. *J. Med. Chem.* **2006**, *49*(2), 534-553.

52. Sotriffer, C. A. *Curr Top Med Chem.* **2011**, *11*(2), 179-191.

53. Cheung, J.; Gary, E. N.; Shiomi, K.; & Rosenberry, T. L. *ACS Med. Chem. Lett.* **2013***, 4*(11), 1091-1096.

54. Lipinski, C. A.; Lombardo, F.; Dominy, B. W.; & Feeney, P. J. Adv. Drug Delivery Rev., **1997**, 23(1-3), 3-25.

55. Aguirre, G.; Cerecetto, H.; Di Maio, R.; González, M.; Alfaro, M. E. M.; Jaso, A.; Monge-Vega, A. *Bioorg. Med. Chem. Lett.* **2004***, 14*(14), 3835-3839.

56. Singh, S.; Das, T.; Awasthi, M.; Pandey, V. P.; Pandey, B.; & Dwivedi, U. N. *Biotechnol. Appl. Biochem.* **2016**, 63(1), 125-137.

57. Hanada, S.; Yuasa, A.; Kuroiwa, H.; Motoyama, Y.; Nagashima H. *Eur. J. Org. Chem.* **2010**, 1021-1025.

58. Velcicky, J.; Soicke, A.; Steiner, R.; Schmalz, H. G. *J. Am. Chem. Soc.* **2011**, *133*, 6948-6951.

59. Magnus, N. A.; Astleford, B. A.; Brennan, J.; Stout, J. R.; Tharp-Taylor, R. W. *Org. Proc. Res. Dev.* **2009**, *13*, 280-284.

60. Koenig, S. G.; Vandenbossche, C. P.; Zhao, H.; Mousaw, P.; Singh, S. P.; Bakale, R. P. *Org. Lett.* **2009**, *11*, 433-436.

61. Verpoorte, J.A.; Mehta, S.; Edsall, J.T. *J. Biol. Chem.* **1967**, *242*, 184221-184229.

62. Lolak, N.; Akocak, S.; Turkes, C.; Taslimi, P.; Işık, M.; Beydemir, Ş.; Gulçin, İ.; Durgun, M. *Bioorg. Chem.* **2020**, *100*, 103897.

63. Bradford, M. *Anal. Biochem.* **1976**, *72*, 248–254.

64. Lineweaver, H.; Burk, D. *J. Am. Chem. Soc.* **1934**, *56*, 658–666.

65. Demir, Y.; Taslimi, P.; Ozaslan, M.S.; Oztaskın, N.; Çetinkaya, Y.; Gulçin, İ.; Beydemir, S.; Göksu, S. *Arch. Pharm.* **2018**, *351*(12), e1800263.

66. Kocyigit, U.M.; Budak, Y.; Gürdere, M.B.; Tekin, Ş.; Kul Köprülü, T.; Ertürk, F.; Özcan, K.; Gülçin, İ.; Ceylan, M. *Bioorg. Chem.* **2017**, *70*, 118-125.

67. Schrödinger, Maestro, Schrödinger, LLC, New York, **2022**.

68. Schrödinger, SiteMap, Schrödinger, LLC, New York, **2022**.

69. Halgren, T. *Chem. Biol. Drug Des.* **2007**, *69*(2), 146-148.

70. Schrödinger, Protein Preparation, Wizard Schrödinger, LLC, New York, **2022**.

71. DuBay, K. H.; Hall, M. L.; Hughes, T. F.; Wu, C.; Reichman, D. R.; Friesner, R. A. *J. Chem. Theory Comput.* **2012**, *8*(11), 4556-4569.

72. Schroödinger, LigPrep, Schrödinger, LLC, New York, **2022**.

73. Schrödinger, Induced Fit Docking protocol, Glide, Prime, Schrödinger, LLC, New York, **2022**.

74. Schrödinger, QikProp, Schrödinger, LLC, New York, **2022**.